UCSF
UC San Francisco Previously Published Works

Title

Engineered phage-based therapeutic materials inhibit Chlamydia trachomatis intracellular infection

Permalink

https://escholarship.org/uc/item/7g030778

Journal

Biomaterials, 33(20)

ISSN

0267-6605

Authors

Bhattarai, Shanta Raj
Yoo, So Young
Lee, Seung-Wuk
et al.

Publication Date

2012-07-01

DOI

10.1016/j.biomaterials.2012.03.054

Peer reviewed

Engineered phage-based therapeutic materials inhibit *Chlamydia trachomatis* intracellular infection

Shanta Raj Bhattarai [a,b,c,1], So Young Yoo [a,b,c,1], Seung-Wuk Lee [b,c], Deborah Dean [a,b,d,*]

[a] *Center for Immunobiology and Vaccine Development, Children's Hospital Oakland Research Institute, 5700 Martin Luther King Jr. Way, Oakland, CA 94609, USA*
[b] *Department of Bioengineering, University of California, Berkeley, CA 94720, USA*
[c] *Lawrence Berkeley National Laboratory, Berkeley, CA 94720, USA*
[d] *UCSF Department of Medicine, San Francisco, CA 94143, USA*

ABSTRACT

Developing materials that are effective against sexually transmitted pathogens such as *Chlamydia trachomatis* (*Ct*) and HIV-1 is challenging both in terms of material selection and improving bio-membrane and cellular permeability at desired mucosal sites. Here, we engineered the prokaryotic bacterial virus (M13 phage) carrying two functional peptides, integrin binding peptide (RGD) and a segment of the polymorphic membrane protein D (PmpD) from *Ct*, as a phage-based material that can ameliorate *Ct* infection. *Ct* is a globally prevalent human pathogen for which there are no effective vaccines or microbicides. We show that engineered phage stably express both RGD motifs and *Ct* peptides and traffic intracellularly and into the lumen of the inclusion in which the organism resides within the host cell. Engineered phage were able to significantly reduce *Ct* infection in both HeLa and primary endocervical cells compared with *Ct* infection alone. Polyclonal antibodies raised against PmpD and co-incubated with constructs prior to infection did not alter the course of infection, indicating that PmpD is responsible for the observed decrease in *Ct* infection. Our results suggest that phage-based design approaches to vector delivery that overcome mucosal cellular barriers may be effective in preventing *Ct* and other sexually transmitted pathogens.

© 2012 Elsevier Ltd. All rights reserved.

1. Introduction

The cervical and vaginal epithelium are the primary portals of entry for sexually transmitted pathogens such as *Chlamydia trachomatis* (*Ct*), *Neisseria gonorrhea*, herpes simplex virus (HSV), human papilloma virus (HPV) and human immunodeficiency virus (HIV-1). Prevention efforts have focused on vaccine and microbicide development with limited success. Currently, there are only two vaccines for sexually transmitted pathogens, Gardasil and Cervarix, and both target just a few of the high-risk subtypes of HPV [1–4]. Microbicides offer the advantage of preventing both infection and potentially transmission for all strains or subtypes of an organism. In addition, they can be applied vaginally, rectally or orally with or without partner knowledge, the latter of which can be advantageous in high-risk groups such as commercial sex workers where condom use may not be accepted practice [5].

Microbicide materials have been produced in many forms, including gels, creams, suppositories, films, or as a sponge or ring that releases an active ingredient over time. A number of materials have been tried or show promise as microbicide formulations. These include drugs such as tenofovir or other antiretrovirals for HIV-1 [6], monoclonal antibodies (MAb) such as the broadly neutralizing human MAb b12 for HIV-1 [7], DNA administered in a controlled delivery matrix of poly(ethylene-co-vinyl acetate) (EVAc) [8], and small interfering RNA (siRNA) delivered by lipoplexes to target HSV 2 [9] or delivered via poly(lactic-co-glycolic acid) (PLGA) nanoparticles [10]. Recently, PLGA nanoparticles have been used to successfully deliver the antibiotics azithromycin and rifampin into *Chlamydia*-infected cells to decrease bacterial infection [11]. While antibiotic therapy can effectively eliminate most uncomplicated *Ct* infections, follow-up screening of treated patients has revealed that a substantial number fail treatment or develop persistent infections [12–16]. Both of these outcomes are indicative of drug resistance, which would presumably limit the use of antibiotics in microbicides.

* Corresponding author. Children's Hospital & Research Center at Oakland, 5700 Martin Luther King Jr. Way, Oakland, CA 94609, USA. Tel.: +1 510 450 7655; fax: +1 510 450 7910.

E-mail address: ddean@chori.org (D. Dean).

[1] These authors contributed equally to the research.

Drug resistance has certainly been a major issue for *N. gonorrhea* [17] and HIV-1 [18].

Several lytic or virulent (shorter replication cycle) phages (mostly T-phages, T1 to T7) have been developed for 'phage therapy' to treat human bacterial infectious diseases such as salmonellosis, acute and chronic urogenital inflammation, skin ulcers, infectious allergoses, dysentery, and post-surgical wounds [19–21]. Numerous pharmaceutical companies (e.g., Eli Lilly, Abbot Laboratories, Intralytix) have become actively involved in efforts to produce commercial therapeutic phage. Eli Lilly, for example, developed a water-soluble jelly-based phage product (e.g., Staphylo-jel) for treating abscesses, purulent wounds, vaginitis, mastoiditis and respiratory infections. Temperate (long infection cycle) phages, which are unsuitable candidates for natural phage therapy because they do not lyse all of their host cells, have been studied as materials to display active ingredients for targeted therapeutic delivery.

Recently, phage engineering has been greatly expanded for biomedical applications, including tissue engineering and drug delivery [22–24]. Through genetic engineering, M13 phage possess a nanofibrous shape to display various signaling peptides [i.e., RGD (integrin-binding peptide), IKVAV (neural cell stimulating peptides), and DGEA (bone-cell stimulating peptides)] [25,26]. The resulting phage could self-assemble nanofibrous network structures that are very similar to cellular microenvironments. The structures can influence cellular fate by controlling the biochemical and physical cues of the matrices. These phage and their matrices might be useful for developing topical therapeutic materials because the phage can deliver a large payload ($>1.5 \times 10^{13}$ epitopes per cm^2) of therapeutic molecules without compromising the integrity of the phage [27,28].

The coat covering the M13 phage surface enables delivery of multiple therapeutic peptides and proteins. Here, we developed a newly engineered phage to express two functional peptides, RGD and *Ct* associated proteins, as a model system to test the efficacy of the phage constructs in preventing or ameliorating *Ct* infection. *Ct* is a gram-negative obligate intracellular pathogen that is the leading cause of bacterial sexually transmitted diseases (STD) with more than 92 million cases occurring globally each year [29]. There are currently no vaccines or microbicides to prevent *Ct* infection. RGD and *Ct* polymorphic membrane protein (Pmp) D peptides were chosen to be expressed on the pVIII major and pIII minor coat proteins, respectively, of M13 phage. RGD has been shown to be effective in inducing integrin mediated endocytosis, and recent proteomic profiling of *Ct* has suggested that PmpD might be a good candidate for interfering with *Ct* propagation [30]. PmpD is the most conserved protein among the Pmps for all *Ct* strains and *Chlamydia* species [31–34] and may play a role in cell entry [31–33]. It is both an auto transporter (AT) [35] and a species-common pan-neutralizing antigen [36]. We selected a conserved portion of the PmpD protein for expression in M13 phage.

We hypothesized that the resulting modified M13 phage would enhance cellular internalization, hone to the *Ct* inclusion in which the organism resides within the cytoplasm of the cell, and enable a significant reduction in *Ct* infection during the developmental cycle of the organism. Application of this system as a topical therapeutic would constitute a new strategy to prevent or reduce sexually transmitted infections.

2. Materials and methods

2.1. HeLa 229 and primary endocervical (PEC) cell culture

HeLa 229 cells were grown to 70% confluence in 24 well plates (Costar, Corning, NY) in media (MEM [Life Technologies, Grand Island, NY] supplemented with 10% Fetal Bovine Serum [FBS, JR Scientific, Inc., Woodland, CA], 50 µg/mL Vancomycin [Fisher Scientific, Pittsburgh, PA], 10 µg/mL Gentamicin [MP Biomedicals, LLC, Solon, OH], Amphotericin B [MP Biomedicals], and 25 U/mL Nystatin [Sigma, St. Louis, MO]) as we described [37] prior to infection with M13 phage or *Ct*.

Primary endocervical tissue was obtained from Alta Bates Hospital (Berkeley, CA). Because the tissue was designated for discard with no link to patient name, the research was considered non-human subjects according to the rules and regulations of the National Institutes of Health. The primary endocervical tissue explants (~10–20 mm^2 sections) were subdivided into 1–2 mm^2 sections in DMEM media (Life Technologies, Grand Island, NY) and centrifuged at 800 rpm for 3 min. The supernatant was aspirated off and the pellet was resuspended in 10 mL of ACK lysis buffer (Lonza Walkersville, Inc., Walkersville, MD) prior to the addition of 10 mL HBSS (Mediatech, Inc., Manassas, VA) and centrifugation at 800 rpm for 3 min. The pellet was then mixed with 5 mL DMEM containing an enzyme cocktail [1.6 mg/mL Collagenase, 0.1 mg/mL Hyaluronidase, 3.4 mg/mL Pancreatin (all reagents from Sigma)] and incubated for 90 min in a shacking incubator at 180 rpm at 37°C. The tissue was centrifuged at 600 rpm for 15 s and resuspended in 3 mL trypsin (Mediatech, Inc.). The trypsinized tissue was resuspended in 9 mL of PEC cell medium (1:1, v/v, Hams F-12 and Dulbecco modified Eagle medium supplemented with 1% Non-essential amino acids, 10 µg/mL insulin, and 2.5 mM L-glutamine, (UCSF Cell Culture Facility, San Francisco, CA) with 10% Fetal Bovine Serum (FBS, JR Scientific, Inc., Woodland, CA), 50 µg/mL Vancomycin (Fisher Scientific), 10 µg/mL Gentamicin, (MP Biomedicals), Amphotericin B (MP Biomedicals), and 25 U/mL Nystatin (Sigma). The cells were plated in 24 well plates and incubated at 37 °C in 5% CO$_2$. After 72 h, PEC cell medium was replaced every 2–3 days until the cells reached 80% confluence.

2.2. Genetic engineering of M13 phage

To engineer M13 phage major (pVIII) and minor (pIII) coat proteins, an inverse PCR cloning method was adapted [38,39]. M13-RGD$_8$ construction methods were used as described previously (Supplementary Table S1-S2, for primer sequences) [23] using the M13KE phage vector (New England Biolabs, Ipswich, MA). For the M13-RGD$_8$-PmpD$_3$ construct, a slightly altered approach was used. The pIII reverse primer was designed to include the *EagI* restriction site, the insert sequence, and a segment complimentary to the gIII 5′-3′ strand. The pIII forward primer was designed to make the vector linear and was fully complimentary to the engineered gIII 3′-5′ region, including an *EagI* restriction site. To incorporate the gene sequences, polymerase chain reaction (PCR) was performed using Phusion™ High-Fidelity DNA Polymerase, the two primers, and an M13-RGD$_8$ vector. The obtained product was purified on an agarose gel, eluted with spin column purification, digested with *EagI* enzyme (New England Biolabs), and re-circularized overnight at 16 °C with T4 DNA Ligase (New England Biolabs) [40]. The ligated DNA vector was then transformed into XL10-Gold® Ultracompetent bacteria cells (Stratagene, La Jolla, CA), and the amplified plasmid was verified by DNA sequencing at the University of California Berkeley DNA Sequencing Facility (Berkeley, CA). Viability of phage was tested using plaque forming units (pfu), and the stock pfu-titration of 10^{14} pfu/mL was used.

2.3. Ct infection of HeLa and PEC cells with or without phage

Ct reference strain L$_2$/434 was used in all studies. Inclusion forming units (IFU) were determined as follows. Serial two-fold dilutions of an L$_2$/434 culture harvest after gradient purification were inoculated into duplicate 24 well plates (Costar). After incubation for 24 h at 37 °C in 5% CO$_2$, the wells were fixed with methanol and stained with pathfinder reagent (Bio-Rad Laboratories, Redmond, WA) according to the package insert. IFUs were enumerated directly under fluorescent microscopy at 40× by counting 20 representative fields (RF) per well and averaged with the counts from the duplicate well. The titer was then calculated knowing the average IFU per RF, the area of the RF, the area of the well, the volume applied to the well and the dilution factor. The IFU/mL or multiplicity of infection (MOI) was calculated: {[(RF/well) × (IFU/RF) × (well/0.2 mL) × (dilution factor) = IFU/mL] or IFU/mL/total number of cells = MOI]} as we described [41]. An MOI of one was used to infect HeLa cells, as we described in detail [42], and to infect PEC cells in 24 well plates with 12 mm glass coverslips (EMS, Hatfield, PA). Briefly, PEC cells grown to a confluence of 80% were infected with phage and/or *Ct* in PEC cell media at room temperature (RT) on an orbital shaker at 180rpm for 2 h. After infection, the supernatant was replaced with fresh PEC cell media (500 µL/well) containing 100 µg/mL cyclohexamide (Sigma) and incubated at 37°C in 5% CO$_2$ for time points post infection.

A competition assay was performed to determine the effect of M13-RGD$_8$ and M13-RGD$_8$-PmpD$_3$ on *Ct* uptake by HeLa cells. There were three experimental groups consisting of *Ct* alone, and M13-RGD$_8$ or M13-RGD$_8$-PmpD$_3$ incubated with *Ct* prior to infection. Phage were first diluted in 200 µL MEM media to arrive at the above concentrations of 10^{11} pfu/mL prior to incubation with *Ct* strain L$_2$ at an MOI of one in 24 well plates for 1 h or 2 h at RT. The media was removed prior to infecting the HeLa cells with the phage/*Ct* complex or *Ct* alone. Infection was performed as above. Briefly, the plates were incubated for 3 h at RT on an orbital shaker prior to centrifugation at 2000 rpm for 30 min, and then incubated at 37°C in 5% CO2. After 36 h, the cells were fixed and the inclusions for each experiment were visualized under fluorescent microscopy as described above. The results were expressed as percent IFU (% IFU). Each experiment was performed in triplicate.

There were five experimental groups of infection (mock, *Ct* alone, M13 wild type, M13-RGD$_8$ or M13-RGD$_8$-PmpD$_3$ alone, pre-treatment with phage and then *Ct*, and co-treatment of phage and *Ct*) that were performed in triplicate. Mock and *Ct* infections were performed as described above. For pre-treatment, phages were diluted in 200 μL cell media (with respective cell line) to arrive at the above concentrations and incubated with HeLa or PEC cells for 2 h at RT. The media was removed and the cells were infected with *Ct* for 2 h at RT in HeLa media for HeLa cells and PEC cell media for PEC cells. For co-treatment, cells were infected with phage and *Ct* at the same time for 2 h at RT. The media was removed and the plates were incubated at 37°C in 5% CO$_2$. The plates were centrifuged at 2000 rpm for 30 min and incubated for time points post infection. M13 wild type, M13-RGD$_8$ or M13-RGD$_8$-PmpD$_3$ infections were performed using concentrations of 10^6, 10^9, 10^{11} or 10^{12} pfu/mL; pfu was determined by the plaque assay as follows [43,44]: 10 μL of each dilution of infected lysates were added to 90 μL of *E. coli* XL10-Gold in late log phase of growth followed by incubation for 10 min at RT, then mixed with 3 mL of Top-Agar and spread onto ITPG-Xgal-LB plates. Blue plaques were counted after overnight incubation at 37°C. The results of experiments with *Ct* and phage infections were expressed as IFU and pfu, respectively, and normalized against the controls of *Ct* infection alone and phage infection alone, respectively.

2.4. Fluorescent microscopy studies

Fluorescent detection of *Ct* was performed as previously described [37]. Briefly, glass coverslips were removed from each well and fixed with absolute methanol (−20 °C) for 10 min and washed three times with Dulbecco's Phosphate-Buffered Saline (DPBS; Mediatech). For *Ct* inclusion detection, a *Ct* hsp60-specific MAb, (HSP 60; Santa Cruz Biotechnology, Santa Cruz, CA) diluted 1:500 in DPBS, and a Cy-3 conjugated a secondary antibody (Cy™3-conjugated IgG; Jackson Immuno Research Laboratories Inc, West Grove, PA), diluted 1:1000 were used. For phage detection, an M13 phage-specific MAb (Anti-fd Bacteriophage; Sigma) and a secondary Alexa Fluor 488-conjugated secondary antibody, both diluted 1:1000 in DPBS (Invitrogen, Eugene, OR), were used. The coverslips were incubated for 2 h with primary antibodies followed by three washes with DPBS before application of the secondary antibodies for 1 h at RT. Nuclear DNA was stained with 1 μg/mL of 4′, 6-Diamidin-2′-phenylindoldihydrochlorid (DAPI, Invitrogen, Eugene, OR). Images were acquired either by a Nikon Eclipse TE-200 fluorescence microscope or by a ZEISS LSM710 laser-scanning confocal microscope with Bitplane's Imaris Suite for image analysis and 3D reconstruction (Zeiss LSM Image Browser Software, version 3.2, Thornwood, NY) at the CHORI Microimaging facility. For determination of percent IFUs (% IFU), duplicate wells were counted as above to determine the total number of IFUs per total number of cells per well. For confocal imaging, the sections were scanned under oil-immersion at 63×. The z-stack images were reconstructed into z-projections using the projection algorithms in the Zeiss LSM Software. Each experiment was performed in triplicate.

2.5. Cell viability and proliferation with phage exposure tested by WST-1 (water soluble tetrazolium salts) assay

The WST-1 (2-(4-Iodophenyl)-3-(4-nitrophenyl)-5-(2,4-disulfophenyl)-2H-tetrazolium, monosodium salt) assay (Cell Proliferation Reagent WST-1; Roche Applied Science, Basel, Switzerland) was performed as per the manufacturer's instructions. This cell proliferation assay is based on the cleavage of the tetrazolium salt WST-1 to formazan by cellular mitochondrial dehydrogenases. 10 μL of reagent was mixed with 0.1 mL of growth medium and added to HeLa cells incubated with and with out phage in 96 well plates. The difference between the absorbance at 450 and 690 nm of the medium was read on an ELISA reader (Safire, Tecan Group Ltd., Mannedorf, Switzerland). Each experiment was performed in triplicate.

2.6. Use of polyclonal antibodies to block M13-RGD$_8$-PmpD$_3$ uptake by HeLa and PEC cells

Polyclonal antibodies (Poly-Ab; YenZym, South San Francisco, CA) raised in rabbits against the PmpD peptide (*C. trachomatis* amino acid # 76—93) were used in the following experiments. A triplicate co-treatment experimental design was set up for six different groups: *Ct* alone, *Ct* with Poly-Ab (60%, v/v), *Ct* with M13-RGD$_8$ or M13-RGD$_8$-PmpD$_3$, and *Ct* with Poly-Ab (60%, v/v) complexed M13-RGD$_8$ or M13-RGD$_8$-NpmpD$_3$ using HeLa or PEC cells in 24 well plates. The Poly-Ab (60%, v/v) and M13-RGD$_8$ or M13-RGD$_8$-PmpD$_3$ at a concentration of 10^{11} pfu/mL were incubated for 1 h at 37°C in PBS at RT. The reaction mixture was centrifuged at 1,200 rpm for 1 h at RT and washed two times with DPBS followed by repeat centrifugation (to ensure removal of all non-bound Poly-Ab with phage in the supernatant) prior to co-infecting the cells with the complex and *Ct* at an MOI of one at RT for 2 h. The controls included *Ct* infection at an MOI of one alone, *Ct* plus Poly-Ab (60%, v/v), *Ct* plus M13-RGD$_8$, and *Ct* plus M13-RGD$_8$-PmpD$_3$. HeLa or PEC cells at a confluence of 80% in 24 well plates with coverslips were infected as described above. After 36 h, the inclusions for each experiment were visualized under fluorescent microscopy as described above. The results were expressed as % IFU. Each experiment was performed in triplicate.

2.7. Statistical analysis

Results are presented as mean ± SD. Differences between the groups were analyzed by the Student *t* test or ANOVA when appropriate. Significance was defined as a value of $p < 0.05$.

3. Results

3.1. Genetic engineering of M13 phage engineering

We constructed a phage to express both a eukaryotic cell adhesion motif and a *Ct* peptide. Using recombinant DNA techniques, we genetically engineered M13 phage to display the desired fusion proteins or peptides on their coat surface protein. The phage were engineered with the RGD-integrin binding peptide on pVIII (termed M13-RGD$_8$) to facilitate internalization into eukaryotic cells through integrin mediated endocytosis [45]. For the therapeutic purpose, the *Ct* specific peptide PmpD was engineered on pIII of M13-RGD$_8$ (termed M13-RGD$_8$-PmpD$_3$) to interrupt *Ct* infection and replication. Supplementary Fig. 1 shows confirmation of the DNA sequences and locations for both RGD and the PmpD peptide. The resulting phage displayed a high density of RGD-signaling peptides ($\sim 1.5 \times 10^{13}$ epitopes/cm^2) on the major coat proteins and five copies of the PmpD peptides on the pIII minor coat proteins, respectively (Fig. 1). We used engineered phage with only RGD on pVIII (M13-RGD$_8$) or wild type (without PmpD) as controls.

3.2. Enhanced uptake of M13-RGD$_8$ by HeLa 229 cells

RGD-mediated phage internalization by various cells has been well reported [46—48]. The effect of HeLa 229 cell uptake of wild type (WT) vs M13-RGD$_8$ phage was compared in three independent experiments. The phage were quantified using a plaque forming assay and immunofluorescent microscopy was used to compare both qualitative and quantitative cellular uptake. M13-RGD$_8$ modification resulted in a significant increased uptake by HeLa cells compared to WT (Fig. 2A, $\sim 76.4\%$ at 24 h; $p < 0.0001$; Fig. 2B), and was greater than M13-RGD$_8$ modification on pIII alone (not shown), likely because pVIII has 2700 copies, which is 99% of its protein coat surface [23,49—51]. Titers of internalized phage showed that the recovered M13-RGD$_8$ was viable and able to infect the bacterial host cells (*E. Coli*) up to day 2 and then decreased significantly after that time (Fig. 2A).

When we treated cells with different concentrations of M13-RGD$_8$ (10^6, 10^9, 10^{12} pfu/mL) to determine the saturation uptake effect at different time intervals, there was increasing internalization at higher pfu/mL values with an uptake saturation of 10^{12} pfu/mL phage at 24 h, suggesting that internalization occurs in a dose-dependent manner via integrin-mediated endocytosis of the RGD-engineered phage (Supplementary Fig. 2).

3.3. Effect of M13-RGD$_8$ phage uptake on Ct infection in HeLa cells

To determine whether M13-RGD$_8$ can be internalized into *Ct* infected HeLa cells and interfere with the growth and development of the organism, we pre-treated HeLa cells with M13-RGD$_8$ (10^9 pfu/mL) for 2 h prior to infecting the cells with *Ct* strain L$_2$ at a MOI of one or co-infected the cells with M13-RGD$_8$ and *Ct* at the same concentrations. Both experimental methods resulted in HeLa cell uptake of M13-RGD$_8$ as shown at 36 h post infection (Fig. 3C and D); the controls of HeLa cells infected with *Ct* alone or M13-RGD$_8$ alone are shown in Fig. 3A and B, respectively, for the same time point. Quantification of viable M13-RGD$_8$ by the plaque assay after uptake by HeLa cells showed a dramatically higher uptake (pfu/mL) for the co-treatment method compared to M13-RGD$_8$ alone without *Ct*
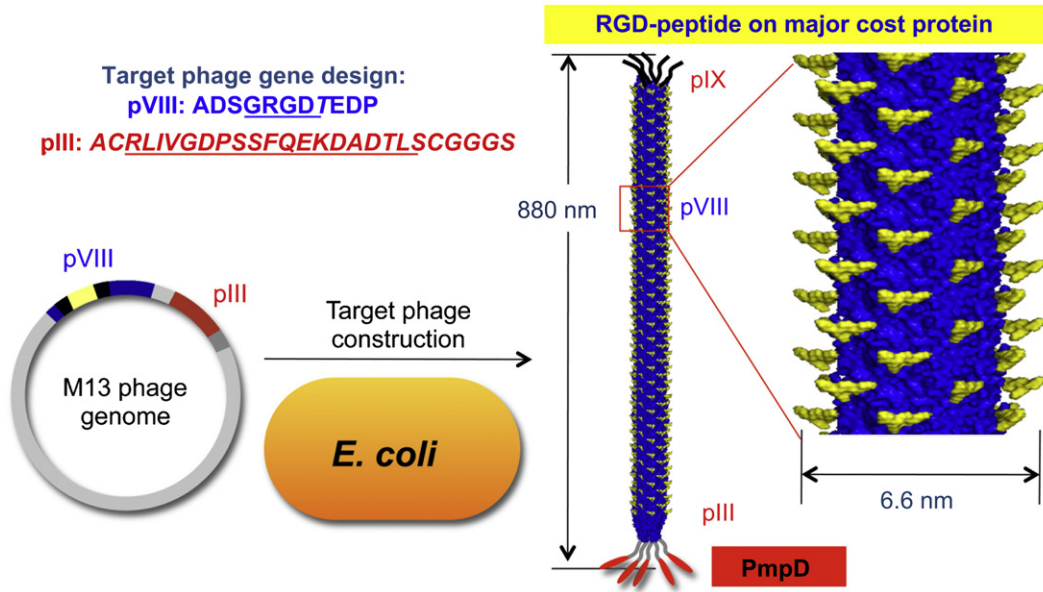
Fig. 1. Schematic of the M13 phage peptide library and gene construction. The phage express high density signaling RGD motifs ($\sim 1.5 \times 10^{13}$ epitopes/cm^2) on pVIII and PmpD on pIII.

infection (Fig. 3E, $p = 0.0821$), although the results were not statistically significant. Ct infection was quantitated by IFU. There was no significant difference for the pre-treatment method (Fig. 3E, $p = 0.3907$). The data represent three independent experiments.

There were no differences in morphology or size of the inclusions between the pre-treatment or co-treatment groups. In addition, M13-RGD$_8$ was observed to surround the Ct inclusion but not traffic into the inclusion (Fig. 3C and D; inset 3D).

3.4. Reduction of Ct infection in HeLa and PEC cells by M13-RGD$_8$-PmpD$_3$

Because PmpD is an AT and pan-neutralizing antigen likely involved in cell entry, we hypothesized that PmpD might interact with the host-pathogen network and possibly block the growth and

development of Ct. To test the first part of this hypothesis, we determined whether M13-RGD$_8$-PmpD$_3$ could inhibit Ct entry into HeLa cells using a competition assay. Supplementary Fig. 3 shows that there was no significant evidence for this either at 1 h or 2 h of incubation prior to infection.

Next, we pre-treated or co-infected HeLa cells as well as PEC cells with M13-RGD$_8$-PmpD$_3$ using the same conditions as above; Ct and M13-RGD$_8$-PmpD$_3$ infections alone were used as controls. PEC cells were selected because they represent cells that have not been laboratory adapted and are physiologically similar to the $in vivo$ endocervical environment, providing an opportunity to pre-clinically validate our findings. There was a significant decrease in Ct infection in both pre-treated and co-infected HeLa cells compared with Ct alone (Fig. 4A). The effect of M13-RGD$_8$-PmpD$_3$ on Ct infection was even more dramatic in PEC cells for pre-
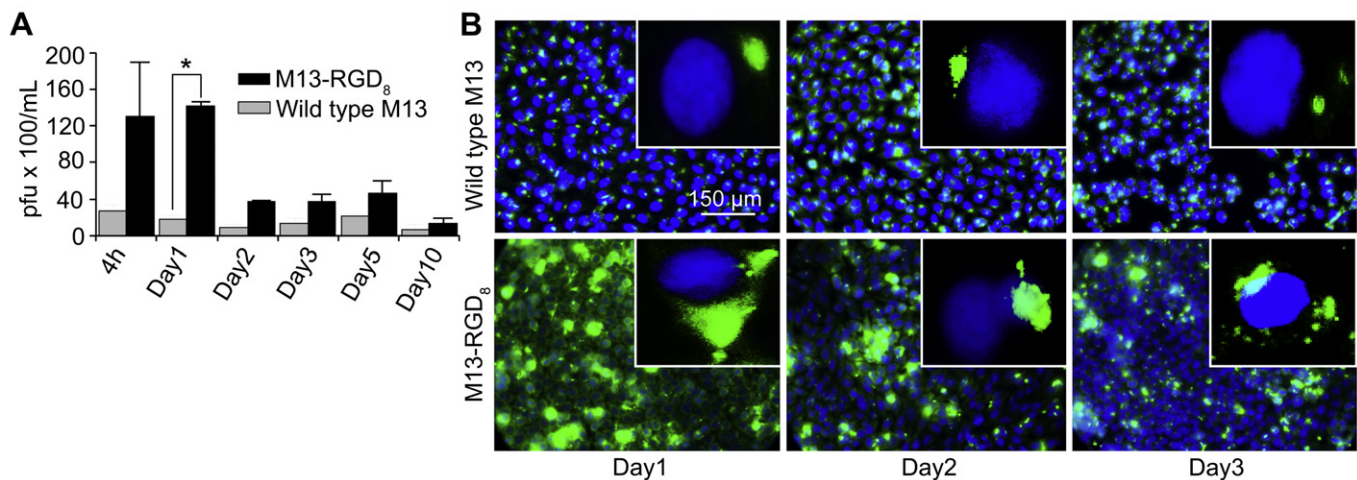

Fig. 2. M13-RGD$_8$ uptake in HeLa 229 cells is significantly higher than for WT M13 phage. (A) Quantitated titers of internalized M13-RGD$_8$ (RGD modification on pVIII protein of M13 phage) in HeLa cells compared with wild type (WT, unmodified M13 phage) show that the recovered M13-RGD$_8$ was viable and able to infect the bacterial host cells (E. Coli) up to day 2 and then decreased dramatically after that time to day 10 (pfu, plaque forming unit; *, $p < 0.0001$). (B) Uptake is significantly higher in M13-RGD$_8$ infected cells and peaks at day 1 compared with WT M13 phage. Blue, DAPI; Green, M13-RGD$_8$; 40×; inset, 100×. Data represent three independent experiments. (For interpretation of the references to colour in this figure legend, the reader is referred to the web version of this article.)
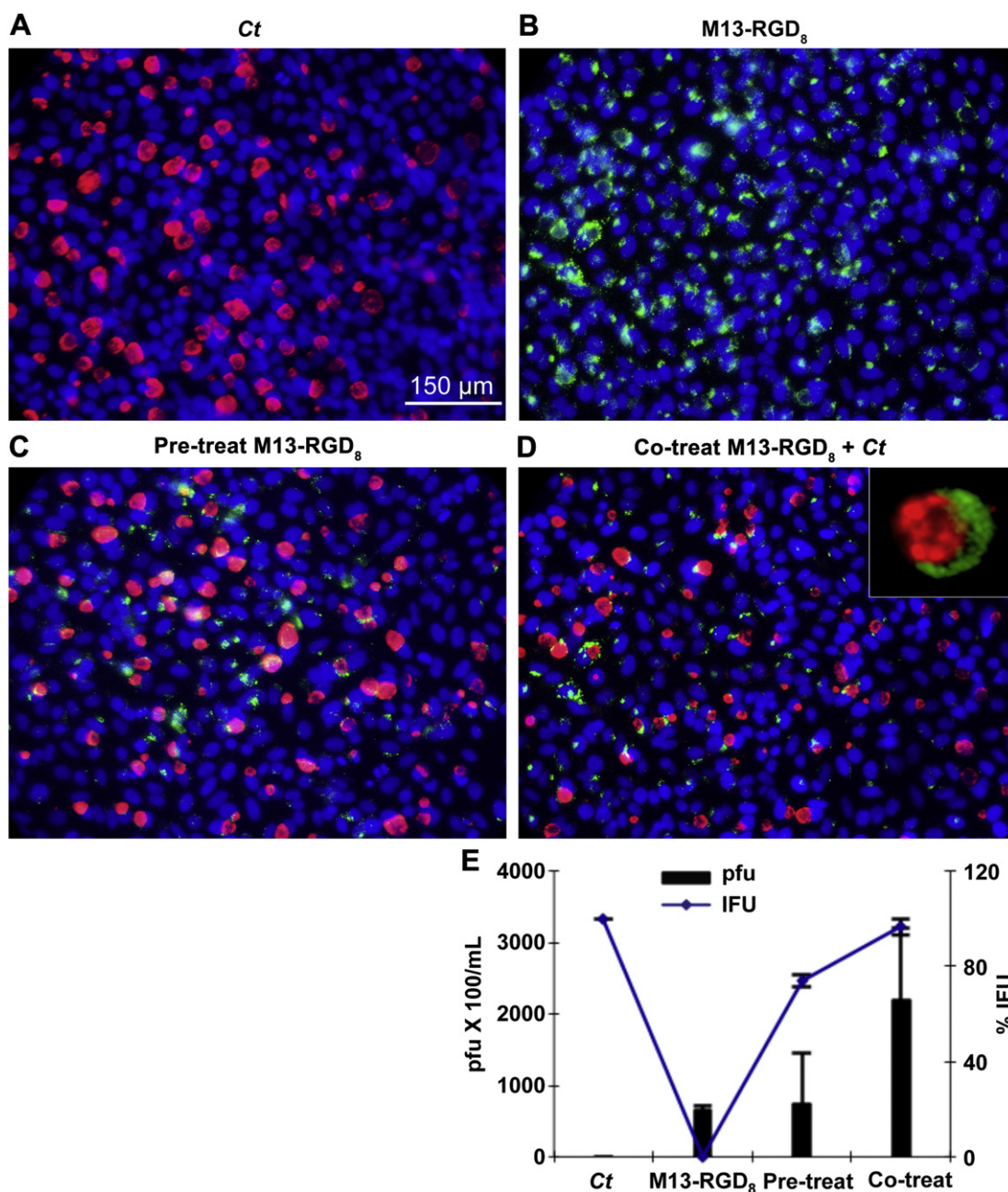
Fig. 3. M13-RGD$_8$ is efficiently internalized by HeLa cells prior to or during infection with *Ct*. (A) Infection of HeLa cells with *Ct* reference strain L$_2$ at an MOI of one; (B) Infection of HeLa cells with M13-RGD$_8$ at a concentration of 10^9 pfu/mL; (C) Pre-treatment of HeLa cells with M13-RGD$_8$ for 2 h prior to *Ct* infection using the same MOI and pfu as in A and B, respectively; and (D) Co-treatment of HeLa cells with M13-RGD$_8$ and *Ct*. (D, Inset) *Ct* inclusion surrounded by M13-RGD$_8$. Blue, DAPI (nuclei); Green, M13-RGD$_8$; Red, *Ct* (red, magenta). 40×; inset, 100×. (E) Quantitated titers of M13-RGD$_8$ uptake (*y*-axis, left) and quantitated *Ct* IFU (*y*-axis, right) at 36 h post infection show dramatically increased phage and *Ct* viability. Data represent three independent experiments. (For interpretation of the references to colour in this figure legend, the reader is referred to the web version of this article.)

treatment and co-infection (Fig. 4B). Fig. 4C shows significant quantitative inhibition of *Ct* infection by M13-RGD$_8$-PmpD$_3$ in HeLa (black; *$p < 0.001$) and PEC (red hatched; **$p < 0.0001$) cells compared with *Ct* alone as measured by IFUs for the co-treatment experiments. A significant effect was also present for the pre-treatment experiments but to a lesser extent. All of the data represent three independent experiments.

The localization of M13-RGD$_8$-PmpD$_3$ in *Ct* infected PEC cells during the developmental cycle of *Ct* was also analyzed. As shown in Fig. 5A, M13-RGD$_8$-PmpD$_3$ accumulated in the cells around the nucleus and inclusion, and appeared to translocate into the

inclusion lumen by 24–30 h with subsequent bursting of the inclusion by 36 h. In addition, at 36 h post co-infection, few PEC cells were observed to be infected. There was also a difference in the size of the inclusions for M13-RGD$_8$-PmpD$_3$ in both pre- and co-treated experiments compared with *Ct* infection alone (Fig. 5A vs Fig. 5B). Invasion of the *Ct* inclusion in PEC cells by M13-RGD$_8$-PmpD$_3$, but not by M13-RGD$_8$ alone, was confirmed by laser scanning microscopy with orthogonal and Z-stack (*x-z* and *y-z* plane) imaging using a Zeiss LSM 710 confocal microscope (Fig. 5C; red, inclusion; green, M13-RGD$_8$-PmpD$_3$). The vertical and horizontal grey lines in Fig. 5D show the specific localization of M13-RGD$_8$-
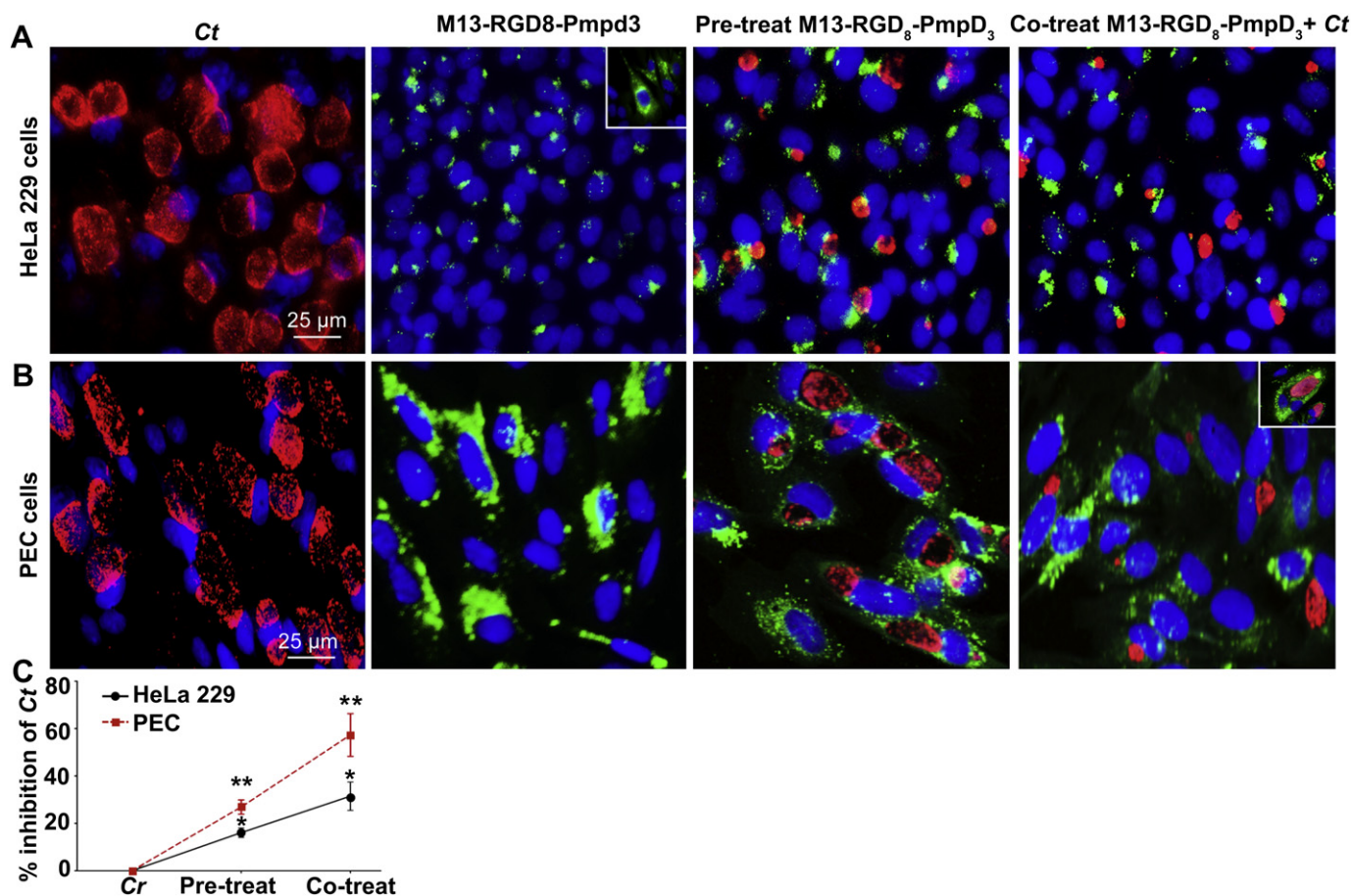
Fig. 4. M13-RGD$_8$-PmpD$_3$ phage are effective in reducing Ct infection in HeLa and primary endocervical (PEC) cells. HeLa and PEC cells were treated with M13-RGD$_8$-PmpD$_3$ (10^{11} pfu/mL) with or without Ct strain L$_2$ at an MOI of one (see Methods). (A) HeLa cells: Ct infection alone; M13-RGD$_8$-PmpD$_3$ alone; Pre-treatment at 2 h with M13-RGD$_8$-PmpD$_3$, and then infection with Ct; and Co-infection with M13-RGD$_8$-PmpD$_3$ and Ct. Inset, phage surrounding the nucleus; (B) PEC cells: same experimental conditions as for HeLa cells. Inset, co-treatment experiment with M13-RGD$_8$-PmpD$_3$ phage surrounding the inclusion of Ct. Blue, DAPI; Green, RGD$_8$-PmpD$_3$; Red/magenta, Ct. 40×; insert, 100×. Data represent three independent experiments; (C) Quantitated results of pre-treatment vs co-infection with M13-RGD$_8$-PmpD$_3$ on Ct infection show significant reduction in Ct infection in HeLa (black) cells and PEC cells (red hatched) compared with Ct infection alone (*, $p < 0.001$; **, $p < 0.0001$, respectively). Data represent three independent experiments. (For interpretation of the references to colour in this figure legend, the reader is referred to the web version of this article.)

PmpD$_3$ within an inclusion, which was not observed for M13-RGD$_8$ (Fig. 5E). Experiments using M13-RGD$_8$-PmpD$_3$ at a concentration of 10^9 pfu/mL showed similar results (not shown).

An *in vitro* cell viability and proliferation assay demonstrated that HeLa cells exposed to M13-RGD$_8$ or M13-RGD$_8$-PmpD$_3$ at a concentration of 10^{11} PFU/mL for various time points had no cytotoxicity compared with untreated cells (Supplementary Fig. 4). HeLa cells exhibited the same proliferation (*$p < 0.01$, two-factor ANOVA) in the presence of M13-RGD$_8$ or M13-RGD$_8$-PmpD$_3$ as for untreated cells. There were similar population numbers (**$p < 0.01$) regardless of phage addition to the media. This is an important observation because it suggests that M13-RGD$_8$ might not be cytopathic in *in vivo* studies.

3.5. No effect on Ct infection in HeLa cells with co-incubation of a polyclonal antibody produced against PmpD with M13-RGD$_8$-PmpD$_3$

We produced a Poly-Ab against PmpD to determine whether it would have a functional effect on Ct infection in HeLa cells with or without M13-RGD$_8$-PmpD$_3$. The Poly-Ab alone was able to significantly inhibit Ct infection by 26.6% (Fig. 6; *, $p = 0.008$) compared with Ct infection alone. When the Poly-Ab was pre-incubated with M13-RGD$_8$-PmpD$_3$ followed by purification of the complex and co-

infected with Ct, there was no significant effect on Ct infection compared with M13-RGD$_8$-PmpD$_3$ without the Poly-Ab. (Fig. 6; **, $p = 0.024$).

4. Discussion

M13 bacteriophage have many features that enable their use as biomedical materials for different therapeutic applications. These include: 1) Safety and lack of toxicity in human cells. Phage are easily removed by the body with few known side-effects [52,53]; 2) Ability to be readily modified to display functional peptide motifs on their minor (pIII, pVI, pVIII and pIX) and major (pVIII) coat proteins. Large quantities of identical phage building blocks can be easily produced by amplification in bacterial host cells; and 3) Ability to form a nanofibrous shape and self-assemble into a nanofibrous matrix that has been used as a vector-mediated therapeutic delivery material for selected tissues [28]. In our previous studies, we used engineered M13 phage in various platforms (e.g., cell assays, cell regeneration and cell fate development) and were able to successfully deliver specific functional peptides into cells and/or matrices [26,50,54,55]. However, functional studies of M13 incorporated peptides (other than ECM derived peptides) and their use in a variety of biomedical applications have not been well studied.
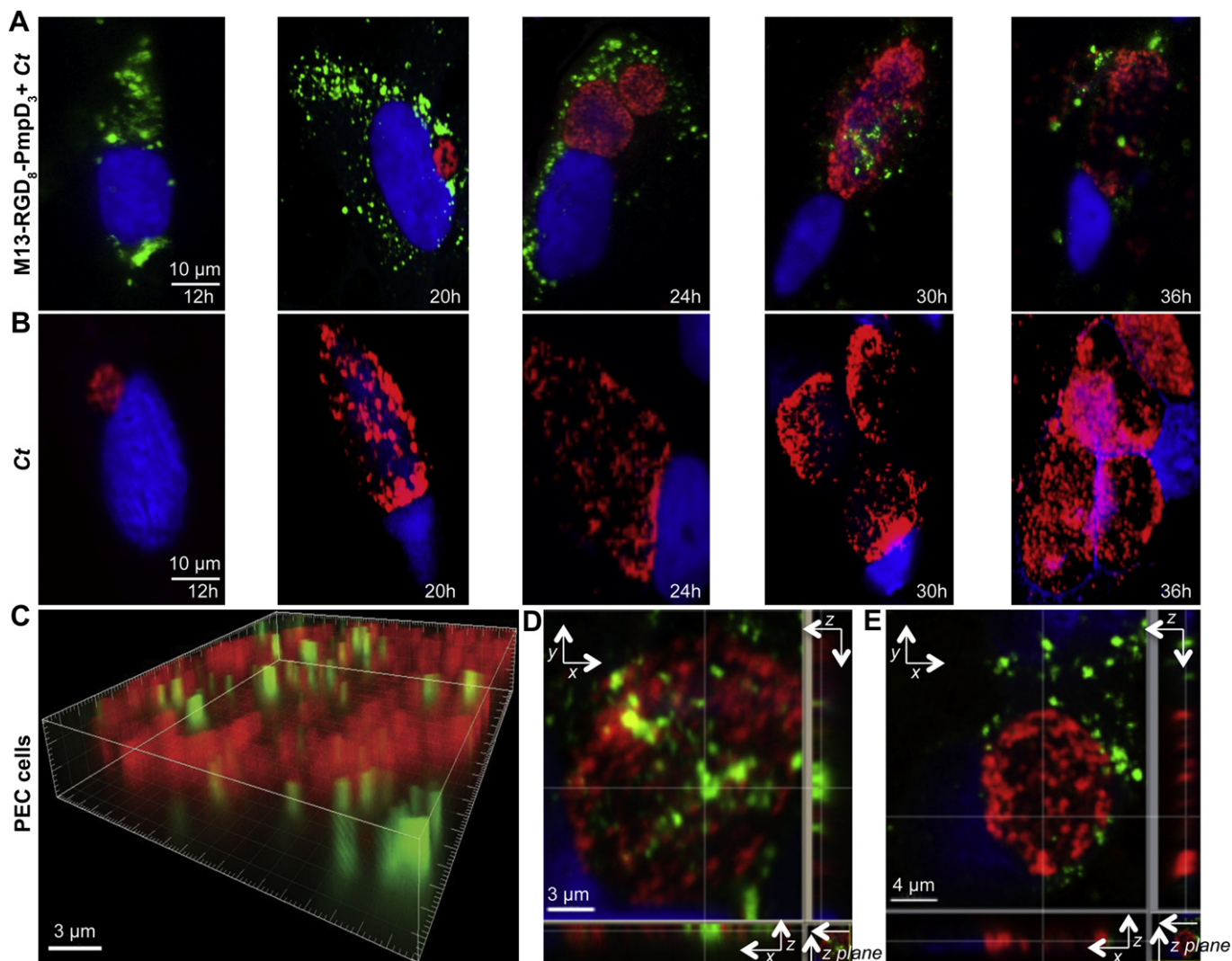
Fig. 5. PEC cells co-treated with M13-RGD$_8$-PmpD$_3$ and *Ct* show trafficking of phage into the inclusion. (A) Timeline from 12 h to 23 h; PEC cells infected with M13-RGD$_8$-PmpD$_3$ at 12 h; inclusion surrounded by phage at 20 h; invasion of the inclusion by M13-RGD$_8$-PmpD$_3$ begins at 24 h and 30 h; disruption of inclusion and dispersal of contents at 36 h. (B) Same timeline as in A except there is no infection with M13-RGD$_8$-PmpD$_3$; the inclusions are visibly larger than in A throughout the developmental cycle of the organism. (C and D) Laser scanning microscopy with orthogonal and 3D projection of Z-stack (*x-z* and *y-z* plane) imaging using a Zeiss LSM 710 confocal microscope; height of field displays an orthogonal slice through a 3D grid showing M13-RGD$_8$-PmpD$_3$ inside the inclusion. (E) laser scanning microscopy with orthogonal Z-stack (*x-z* and *y-z* plane) imaging using a Zeiss LSM 710 confocal microscope; height of field displays an orthogonal slice through a 3D grid showing that M13-RGD$_8$ does not translocate into the lumen of the inclusion. Data represent three independent experiments.

Here, we explored the use of genetically engineered M13 phage as an anti-microbial therapeutic. We believe that our platform of engineered M13 phage (M13-RGD$_8$-PmpD$_3$) could be used as a therapeutic agent at mucosal sites for preventing *Ct* transmission as well as interrupting a new or existing infection. An advantage is that M13 phage that display fusion peptides at the N-terminus of pIII do not interfere with the folding of the globular domains of pIII in contrast to pVIII that can tolerate only short peptides at its N-terminus [25,56]. We showed that by expressing RGD on pVIII, cellular uptake of M13-RGD$_8$ was dramatically enhanced compared with wild type M13 (Fig. 2). Moreover, the addition of PmpD on pIII had no untoward effect on M13-RGD$_8$-PmpD$_3$ uptake (Fig. 4).

The export of *Ct* proteins from within the inclusion to the cytosol to interact with host proteins and initiate various signaling processes are necessary for inhibition of cell death to enable the organism to complete its developmental cycle [57,58]. Through as yet unknown mechanisms, the inclusions traffic to intracellular organelles to sequester host nutrients and lipids for chlamydial replication

[59,60]. Recent studies have shown that the nine member family of Pmps are structurally similar to the AT proteins that have been described for other bacteria [61]. Pmps have also been shown to be involved in cellular and humoral protective immunity against *Ct* infection [62]. Nunes et al. [42] examined the transcription of *Ct* Pmp genes and found that gene expression occurred as early as 2 h and continued throughout the developmental cycle. In other studies, PmpD was shown to initially localize on the surface of the metabolically active reticulate bodies (RB) of *Ct* followed by its cleavage and secretion, suggesting a role for the PmpD protein in transformation from the RB to the infectious inert elementary bodies (EB) [31]. Swanson et al. [35] and Wehrl et al. [32] further showed that PmpD processing involves cleavage of PmpD with initial formation of a passenger domain (PD) followed by cleavage of the PD into two smaller fragments. They demonstrated that PmpD translocates to the surface of bacteria where it non-covalently binds other components of the outer membrane that may function in bacterial invasion and host inflammation. In the present study, we found no significant
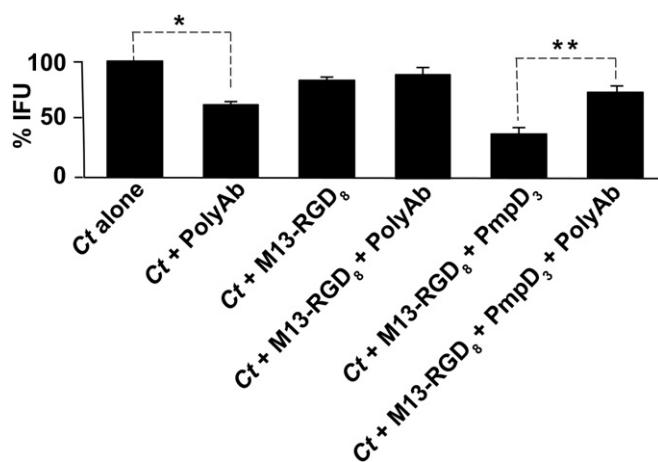
Fig. 6. Polyclonal antibody (Poly-Ab) raised against the PmpD peptide and applied to HeLa cells significantly reduces *Ct* infection. Infection was reduced by 26.6% using the Poly-Ab compared to *Ct* infection alone (*, $p = 0.008$). The Poly-Ab complexed with M13-RGD$_8$PmpD$_3$ and purified prior to co-infection with *Ct* failed to impact infection compared with M13-RGD$_8$PmpD$_3$ alone (**, $p = 0.024$). Data represent three independent experiments.

inhibitory effect of M13-RGD$_8$-PmpD$_3$ on *Ct* entry into HeLa cells compared to *Ct* infection alone or M13-RGD$_8$ alone as demonstrated by a competition assay (Supplementary Fig. 3). This suggests that there may be multiple mechanisms for uptake of *Ct* by the cells and that the phage, if they play any role in this process, do not likely share a common entry pathway or receptor with *Ct* and do not appreciably affect infection of the cell.

The *Ct* inclusion represents the primary barrier between the host and the multiplying organism. The inclusion forms early after the EB penetrates the cell and is comprised of both host and *Ct* proteins [63]. Acquisition of nutrients and other molecules required for *Ct* growth occur through the inclusion [64], although the mechanisms for this exchange remain largely unknown. In this study, we evaluated the effects of the phage constructs on the inclusion and *Ct* infection. Phage were able to enter the host cells and appeared to fill the cytosol; there was no appreciable difference in appearance between M13-RGD$_8$ and M13-RGD$_8$-PmpD$_3$ in terms of distribution within the cytosol. The maximum uptake of the phage was at 24 h, which was dose dependent. We determined by confocal microscopy that M13-RGD$_8$-PmpD$_3$ was translocated from the host cytoplasm into the inclusion lumen and disrupted the inclusion (Fig. 5A, C and D) earlier in the developmental cycle compared with *Ct* infection alone (Fig. 5B). Importantly, M13-RGD$_8$ was not able to penetrate the inclusion (Fig. 5E). These data suggested that distribution patterns vary between different types of engineered phage and that the nature of the displayed foreign protein may dictate docking at the surface and penetration of the inclusion to intimately associate with the replicating RBs.

We also showed that there was a significant reduction in infection in both HeLa and PEC cells when M13-RGD$_8$-PmpD$_3$ was used to pre-treat the cells prior to *Ct* infection or to co-treat the cells with *Ct* (Fig. 4A, B and C). In PEC cells, there was also a noted decrease in the size of the inclusions before disruption compared with *Ct* infection alone (Fig. 5A vs B). The marked reduction of both inclusion number and size in both pre- and co-treatment experiments suggests that M13-RGD$_8$-PmpD$_3$ may block the acquisition of nutrients from the host cell since this effect was not observed for M13-RGD$_8$ (Fig. 3). However, it is not clear exactly at which stage in development there is an effect or what the mechanism may be.

Intracellular protein-specific peptide interactions have been considered for possible 'protein knockout' that can ultimately cause

inhibition of intracellular organisms if the target protein or peptide is essential [65]. To address the specificity of M13-RGD$_8$-PmpD$_3$ in this process, phage were complexed with a rabbit poly-Ab against PmpD prior to infection of HeLa cells with *Ct*. We found that the M13-RGD$_8$-PmpD$_3$ polyclonal complex had a minimal effect on decreasing *Ct* infection, which was significantly different from M13-RGD$_8$-PmpD$_3$ alone (Fig. 6; $p = 0.024$). In contrast, the polyclonal alone significantly decreased infection (Fig. 5F; $p = 0.008$), which is consistent with the neutralizing effects of PmpD antibodies in other *in vitro* studies [36]. Our findings indicate that M13-RGD$_8$-PmpD$_3$, specifically the foreign peptide PmpD, plays a direct role in interrupting intracellular *Ct* infection. The challenge now will be to deliver sufficient active peptides, perhaps with alternate genetic engineering to display an increased number of the protein moieties on multiple surface coat proteins such as pIII, pVIII, and pIX without altering protein folding, to reach 100% inhibition of infection. That said, the fact that over 50% of the infection could be controlled with our current M13-RGD$_8$-PmpD$_3$ construct (Fig. 5D), especially in PEC cells that represent a more physiologically relevant experimental model compared with established cell lines for the *in vivo* endocervical environment, suggests that this approach will likely be successful in preventing *Ct* transmission and ablating existing infection at mucosal sites of infection.

5. Conclusions

We genetically engineered M13 phage to stably express the integrin binding protein RGD and the *Ct* peptide PmpD. This construct, M13-RGD$_8$-PmpD$_3$, was able to ameliorate *Ct* infection in both HeLa cells, an established cell line, and PEC cells that have not been laboratory adapted and are physiologically similar to the *in vivo* endocervical environment. The effect in PEC cells was greater than in HeLa cells. M13-RGD$_8$-PmpD$_3$ was observed to traffic into the lumen of the inclusion unlike the phage construct M13-RGD$_8$, suggesting that this specific construct may be able to hone to the inclusion. In addition, PEC cells treated with M13-RGD$_8$-PmpD$_3$ showed a marked diminution in inclusion size and early disruption of the inclusion compared with *Ct* infection alone, indicating a possible role in blocking nutrient accessibility to the inclusion. While the competition assay using M13-RGD$_8$-PmpD$_3$ pre-incubated with *Ct* did not show any effect on *Ct* entry into the cells, the polyclonal antibodies raised against PmpD prevented the effects of M13-RGD$_8$-PmpD$_3$ on decreasing infection in HeLa cells. Thus, it appears that PmpD plays a direct role in ameliorating *Ct* infection. The precise mechanisms involved will require further study. We present a therapeutic approach to vector delivery that could be expanded for use in a microbicide formulation. Moreover, our approach obviates the need for antibiotics that may induce resistance over time. Carefully engineered M13 phage will likely be successful in not just preventing *Ct* transmission and ablating infection at mucosal sites but provide a model for controlling other sexually transmitted pathogens.

Appendix A. Supplementary material

Supplementary data related to this article can be found online at doi:10.1016/j.biomaterials.2012.03.054.

References

[1] Centers for Disease Control and Prevention. *Human Papillomavirus* (HPV) vaccine. Online. Available from: http://www.cdc.gov/std/stats; 2011.

[2] Romanowski B. Long term protection against cervical infection with the human papillomavirus: review of currently available vaccines. Hum Vaccines 2011;7:161–9.

[3] Kreimer AR, Rodriguez AC, Hildesheim A, Herrero R, Porras C, Schiffman M, et al. Proof-of-principle evaluation of the efficacy of fewer than three doses of a bivalent HPV16/18 vaccine. J Natl Cancer Inst 2011;103:1444–51.

[4] Rappuoli R, Mandl CW, Black S, De Gregorio E. Vaccines for the twenty-first century society. Nat Rev Immunol 2011;11:865–72.

[5] Foss AM, Hossain M, Vickerman PT, Watts CH. A systematic review of published evidence on intervention impact on condom use in sub-Saharan Africa and Asia. Sex Transm Infect 2007;83:510–6.

[6] Abdool Karim Q, Abdool Karim SS, Frohlich JA, Grobler AC, Baxter C, Mansoor LE, et al. Effectiveness and safety of tenofovir gel, an antiretroviral microbicide, for the prevention of HIV infection in women. Science 2010;329:1168–74.

[7] Veazey RS, Shattock RJ, Pope M, Kirijan JC, Jones J, Hu Q, et al. Prevention of virus transmission to macaque monkeys by a vaginally applied monoclonal antibody to HIV-1 gp120. Nat Med 2003;9:343–6.

[8] Shen H, Goldberg E, Saltzman WM. Gene expression and mucosal immune responses after vaginal DNA immunization in mice using a controlled delivery matrix. J Control Release 2003;86:339–48.

[9] Palliser D, Chowdhury D, Wang QY, Lee SJ, Bronson RT, Knipe DM, et al. An siRNA-based microbicide protects mice from lethal herpes simplex virus 2 infection. Nature 2006;439:89–94.

[10] Woodrow KA, Cu Y, Booth CJ, Saucier-Sawyer JK, Wood MJ, Saltzman WM. Intravaginal gene silencing using biodegradable polymer nanoparticles densely loaded with small-interfering RNA. Nat Mater 2009;8:526–33.

[11] Toti US, Guru BR, Hali M, McPharlin CM, Wykes SM, Panyam J, et al. Targeted delivery of antibiotics to intracellular chlamydial infections using PLGA nanoparticles. Biomaterials 2011;32:6606–13.

[12] Somani J, Bhullar VB, Workowski KA, Farshy CE, Black CM. Multiple drug-resistant *Chlamydia trachomatis* associated with clinical treatment failure. J Infect Dis 2000;181:1421–7.

[13] Bhengraj AR, Vardhan H, Srivastava P, Salhan S, Mittal A. Decreased susceptibility to azithromycin and doxycycline in clinical isolates of *Chlamydia trachomatis* obtained from recurrently infected female patients in India. Chemotherapy 2010;56:371–7.

[14] Horner P. The case for further treatment studies of uncomplicated genital *Chlamydia trachomatis* infection. Sex Transm Infect 2006;82:340–3.

[15] Dean D, Suchland RJ, Stamm WE. Evidence for long-term cervical persistence of *Chlamydia trachomatis* by omp1 genotyping. J Infect Dis 2000;182:909–16.

[16] Hogan RJ, Mathews SA, Mukhopadhyay S, Summersgill JT, Timms P. Chlamydial persistence: beyond the biphasic paradigm. Infect Immun 2004;72:1843–55.

[17] Ison CA. Antimicrobial resistance in sexually transmitted infections in the developed world: implications for rational treatment. Curr Opin Infect Dis; 2011.

[18] Wood E, Montaner JS. Time to get serious about HIV antiretroviral resistance. Lancet Infect Dis 2011;11:723–4.

[19] Abedon ST, Kuhn S, Blasdel B, Kutter EM. Phage treatment of human infections (invited review). Bacteriophage 2011;1:66–85.

[20] Kutter E, De Vos D, Gvasalia G, Alavidze Z, Gogokhia L, Kuhl S, et al. Phage therapy in clinical practice: treatment of human infections. Curr Pharm Biotechnol 2010;11:69–86.

[21] Westwater C, Kasman LM, Schofield DA, Werner PA, Dolan JW, Schmidt MG, et al. Use of genetically engineered phage to deliver antimicrobial agents to bacteria: an alternative therapy for treatment of bacterial infections. Antimicrob Agents Chemother 2003;47:1301–7.

[22] Chung WJ, Oh JW, Kwak K, Lee BY, Meyer J, Wang E, et al. Biomimetic self-templating supramolecular structures. Nature 2011;478:364–8.

[23] Merzlyak A, Indrakanti S, Lee SW. Genetically engineered nanofiber-like viruses for tissue regenerating materials. Nano Lett 2009;9:846–52.

[24] Lee SW, Mao C, Flynn CE, Belcher AM. Ordering of quantum dots using genetically engineered viruses. Science 2002;296:892–5.

[25] Smith GP, Petrenko VA. Phage display. Chem Rev 1997;97:391–410.

[26] Yoo S-Y, Merzlyak A, Lee S- W. Facile growth factor immobilization platform based on engineered phage matrices. Soft Matter 2011;7:16601666.

[27] Poul MA, Marks JD. Targeted gene delivery to mammalian cells by filamentous bacteriophage. J Mol Biol 1999;288:203–11.

[28] Frenkel D, Solomon B. Filamentous phage as vector-mediated antibody delivery to the brain. Proc Natl Acad Sci U S A 2002;99:5675–9.

[29] World Health Organization. Initiative for vaccine research. Online. Available from: http://www.who.int/vaccine_research/diseases/soa_std/en/index1.htmL; 2011.

[30] Kariagina AS, Alekseevskii AV, Spirin SA, Zigangirova NA, Gintsburg AL. Effector proteins of *Chlamydia*. Mol Biol (Mosk) 2009;43:963–83.

[31] Kiselev AO, Skinner MC, Lampe MF. Analysis of pmpD expression and PmpD post-translational processing during the life cycle of *Chlamydia trachomatis* serovars A, D, and L2. PLoS One 2009;4:e5191.

[32] Wehrl W, Brinkmann V, Jungblut PR, Meyer TF, Szczepek AJ. From the inside out—processing of the Chlamydial autotransporter PmpD and its role in bacterial adhesion and activation of human host cells. Mol Microbiol 2004;51:319–34.

[33] Wells TJ, Tree JJ, Ulett GC, Schembri MA. Autotransporter proteins: novel targets at the bacterial cell surface. FEMS Microbiol Lett 2007;274:163–72.

[34] Kiselev AO, Stamm WE, Yates JR, Lampe MF. Expression, processing, and localization of PmpD of *Chlamydia trachomatis* Serovar L2 during the chlamydial developmental cycle. PLoS One 2007;2:e568.

[35] Swanson KA, Taylor LD, Frank SD, Sturdevant GL, Fischer ER, Carlson JH, et al. *Chlamydia trachomatis* polymorphic membrane protein D is an oligomeric autotransporter with a higher-order structure. Infect Immun 2009;77:508–16.

[36] Crane DD, Carlson JH, Fischer ER, Bavoil P, Hsia RC, Tan C, et al. *Chlamydia trachomatis* polymorphic membrane protein D is a species-common pan-neutralizing antigen. Proc Natl Acad Sci U S A 2006;103:1894–9.

[37] Somboonna N, Wan R, Ojcius DM, Pettengill MA, Joseph SJ, Chang A, et al. Hypervirulent *Chlamydia trachomatis* clinical strain is a recombinant between lymphogranuloma venereum (L$_2$) and D lineages. mBio 2011;2. p. e00045–11.

[38] Chen G, Courey AJ. Generation of epitope-tagged proteins by inverse PCR mutagenesis. Biotechniques 1999;26:814–6.

[39] Qi D, Scholthof KB. A one-step PCR-based method for rapid and efficient site-directed fragment deletion, insertion, and substitution mutagenesis. J Virol Methods 2008;149:85–90.

[40] Sambrook J, Russell DW. Molecular Cloning: a laboratory manual. 3rd ed. Plainview, NY: Cold Spring Harbor Laboratory Press; 2001.

[41] Somboonna N, Mead S, Liu J, Dean D. Discovering and differentiating new and emerging clonal populations of *Chlamydia trachomatis* with a novel shotgun cell culture harvest assay. Emerg Infect Dis 2008;14:445–53.

[42] Nunes A, Gomes JP, Mead S, Florindo C, Correia H, Borrego MJ, et al. Comparative expression profiling of the *Chlamydia trachomatis* pmp gene family for clinical and reference strains. PLoS One 2007;2:e878.

[43] Gratia A. Numerical relations between lysogenic bacteria and particles of bacteriophage. Ann Inst Pasteur 1936;57:652–76.

[44] Hershey AD, Kalmanson G, Bronfenbrenner H. Quantitative methods in the study of the phage-antiphage reaction. J Immunol 1943;46:267–79.

[45] Erbacher P, Remy JS, Behr JP. Gene transfer with synthetic virus-like particles via the integrin-mediated endocytosis pathway. Gene Ther 1999;6:138–45.

[46] Hart SL, Knight AM, Harbottle RP, Mistry A, Hunger HD, Cutler DF, et al. Cell binding and internalization by filamentous phage displaying a cyclic Arg-Gly-Asp-containing peptide. J Biol Chem 1994;269:12468–74.

[47] Kassner PD, Burg MA, Baird A, Larocca D. Genetic selection of phage engineered for receptor-mediated gene transfer to mammalian cells. Biochem Biophys Res Commun 1999;264:921–8.

[48] Shayakhmetov DM, Eberly AM, Li ZY, Lieber A. Deletion of penton RGD motifs affects the efficiency of both the internalization and the endosome escape of viral particles containing adenovirus serotype 5 or 35 fiber knobs. J Virol 2005;79:1053–61.

[49] Chung WJ, Merzlyak A, Yoo SY, Lee SW. Genetically engineered liquid-crystalline viral films for directing neural cell growth. Langmuir 2010;26: 9885–90.

[50] Yoo SY, Chung WJ, Kim TH, M. L, Lee SW. Facile patterning of genetically engineered M13 bacteriophage for directional growth of human fibroblast cells. Soft Matter 2011;7:363–8.

[51] Wang YA, Yu X, Overman S, Tsuboi M, Thomas Jr GJ, Egelman EH. The structure of a filamentous bacteriophage. J Mol Biol 2006;361:209–15.

[52] Projan S. Phage-inspired antibiotics? Nat Biotechnol 2004;22:167–8.

[53] Merril CR, Biswas B, Carlton R, Jensen NC, Creed GJ, Zullo S, et al. Long-circulating bacteriophage as antibacterial agents. Proc Natl Acad Sci U S A 1996;93:3188–92.

[54] Yoo SY, Kobayashi M, Lee PP, Lee SW. Early osteogenic differentiation of mouse preosteoblasts induced by collagen-derived DGEA-peptide on nanofibrous phage tissue matrices. Biomacromolecules 2011;12:987–96.

[55] Yoo SY, Oh JW, Lee SW. Phage-chips for novel optically readable tissue engineering assays. Langmuir 2012;28:2166–72.

[56] Petrenko VA, Smith GP, Gong X, Quinn T. A library of organic landscapes on filamentous phage. Protein Eng 1996;9:797–801.

[57] Beeckman DS, Vanrompay DC. Bacterial secretion systems with an emphasis on the chlamydial type III secretion system. Curr Issues Mol Biol 2010;12:17–42.

[58] Ying S, Pettengill M, Ojcius DM, Hacker G. Host-cell survival and death during *Chlamydia* infection. Curr Immunol Rev 2007;3:31–40.

[59] Robertson DK, Gu L, Rowe RK, Beatty WL. Inclusion biogenesis and reactivation of persistent *Chlamydia trachomatis* requires host cell sphingolipid biosynthesis. PLoS Pathog 2009;5:e1000664.

[60] Saka HA, Valdivia RH. Acquisition of nutrients by *Chlamydiae*: unique challenges of living in an intracellular compartment. Curr Opin Microbiol 2010;13: 4–10.

[61] Henderson IR, Lam AC. Polymorphic proteins of *Chlamydia* spp.—autotransporters beyond the Proteobacteria. Trends Microbiol 2001;9:573–8.

[62] Eko FO, Ekong E, He Q, Black CM, Igietseme JU. Induction of immune memory by a multisubunit chlamydial vaccine. Vaccine 2011;29:1472–80.

[63] Fields KA, Hackstadt T. The chlamydial inclusion: escape from the endocytic pathway. Annu Rev Cell Dev Biol 2002;18:221–45.

[64] Heuer D, Rejman Lipinski A, Machuy N, Karlas A, Wehrens A, Siedler F, et al. *Chlamydia* causes fragmentation of the Golgi compartment to ensure reproduction. Nature 2009;457:731–5.

[65] Benson RE, Gottlin EB, Christensen DJ, Hamilton PT. Intracellular expression of Peptide fusions for demonstration of protein essentiality in bacteria. Antimicrob Agents Chemother 2003;47:2875–81.

Supplementary Tables

Table S1

Genetically engineered nanophage used in this study

Name	pVIII	pIII
M13-RGD8	A*DLGRGDTE*DP	
M13-RGD3		SHS*ACGRGDSCGGGS*AET
M13- RGD8-NpmpD3	A*DLGRGDTE*DP	SHS*ACRLIVGDPSSFQEKDADTLSCGGGS*AET
M13	AEGDDP	SHSAET

*Note: Peptide inserts are shown in italic and **bold**. Functional sequences are also <u>underlined</u>.*

Table S2

Primers used for pVIII and pIII engineering

Name	Oligonucleotide Primer Sequence* (5'-3')	Insert Peptide Sequence**
p8-RGD	ATATAT**CTGCAG**_NK(NNK)2CGTGGTGAT(NNK)2_GATCCCG CAAAAGCGGCCTTTAACTC CC	A_XXXRGDXX_DP A_DLGRGDTE_DP ***
p8-rev1376	CCTCTGCAGCGAAAGACAGCATCGG	
p3-NpmpD	TATATA**CGGCCG**A_TCCACCGCC GCACAG GGTATCCGCGTCTTTTTCCTGAAAACTGCTCGGATCGCCCAC AATCAGACG_GCACGCCGAGTGAGAATAGAAAGGAACCA C TAAAGG	SHSAC_RLIVGDPSSFQ EKDADTL_CGGGSAET
p3-Fwd1626	AAACACT **CGGCCG** AAACTGTTGAAAGT TGTTTAGC	

* For primer oligonucleotide sequences the restriction sites are shown in **bold**, and the insert is <u>*underlined and italic*</u>
** For the resulting peptide sequence the insert is <u>*underlined and italic*</u>
*** Constructed from partial library approach,$^{\psi}$ selected sequence indicated

$^{\psi}$ Merzlyak A, Indrakanti S and Lee SW. Genetically engineered nanofiber-like viruses for tissue regenerating materials. *Nano Lett* **9**, 846-852 (2009).
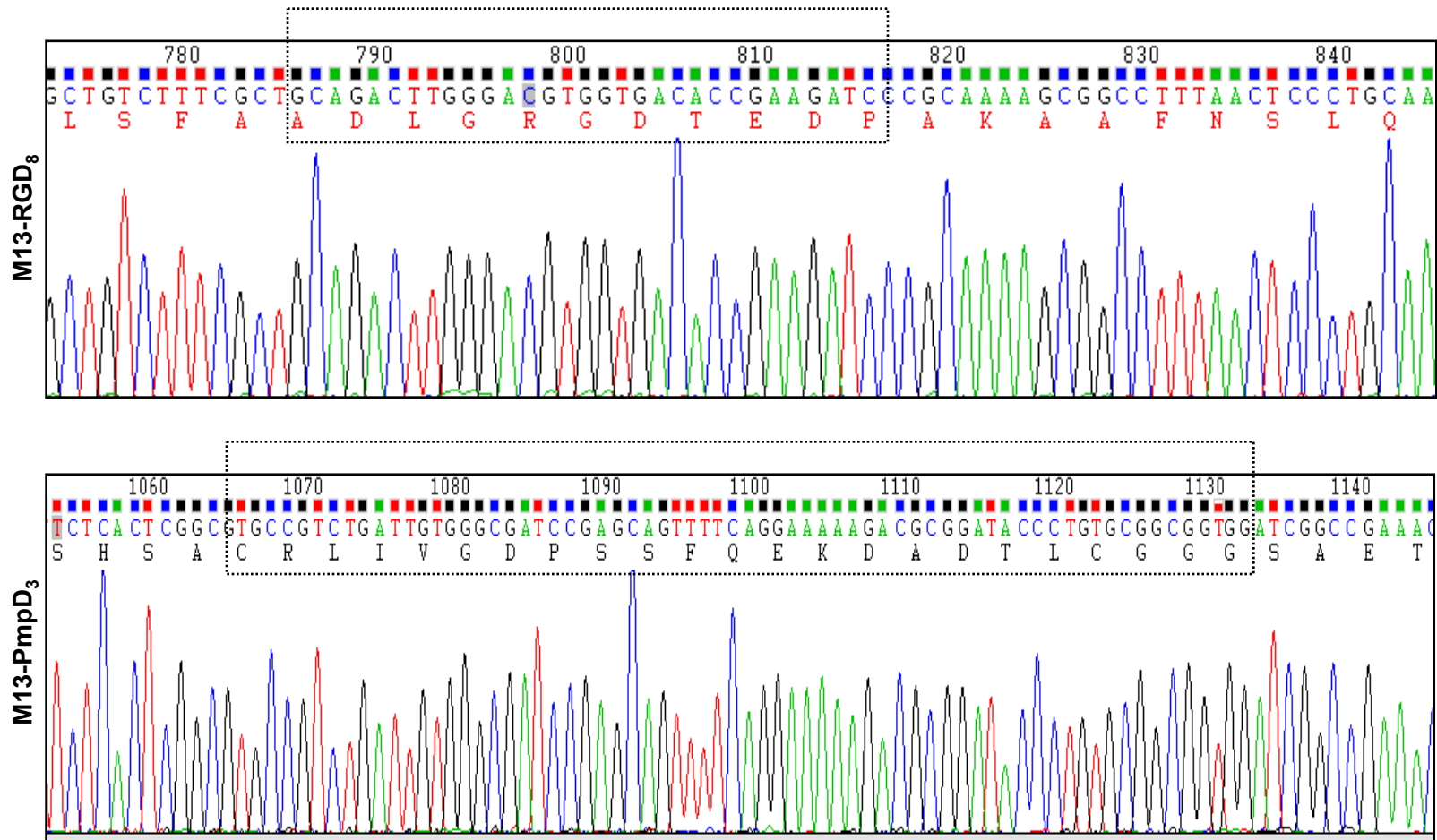
Fig. S1. DNA sequence confirmation and locations of inserts in the M13 phage genome for M13-RGD$_8$ and M13-PmpD$_3$ peptides. M13-RGD$_8$ and M13-PmpD$_3$ were engineered on pVIII and pIII, respectively (see Methods).
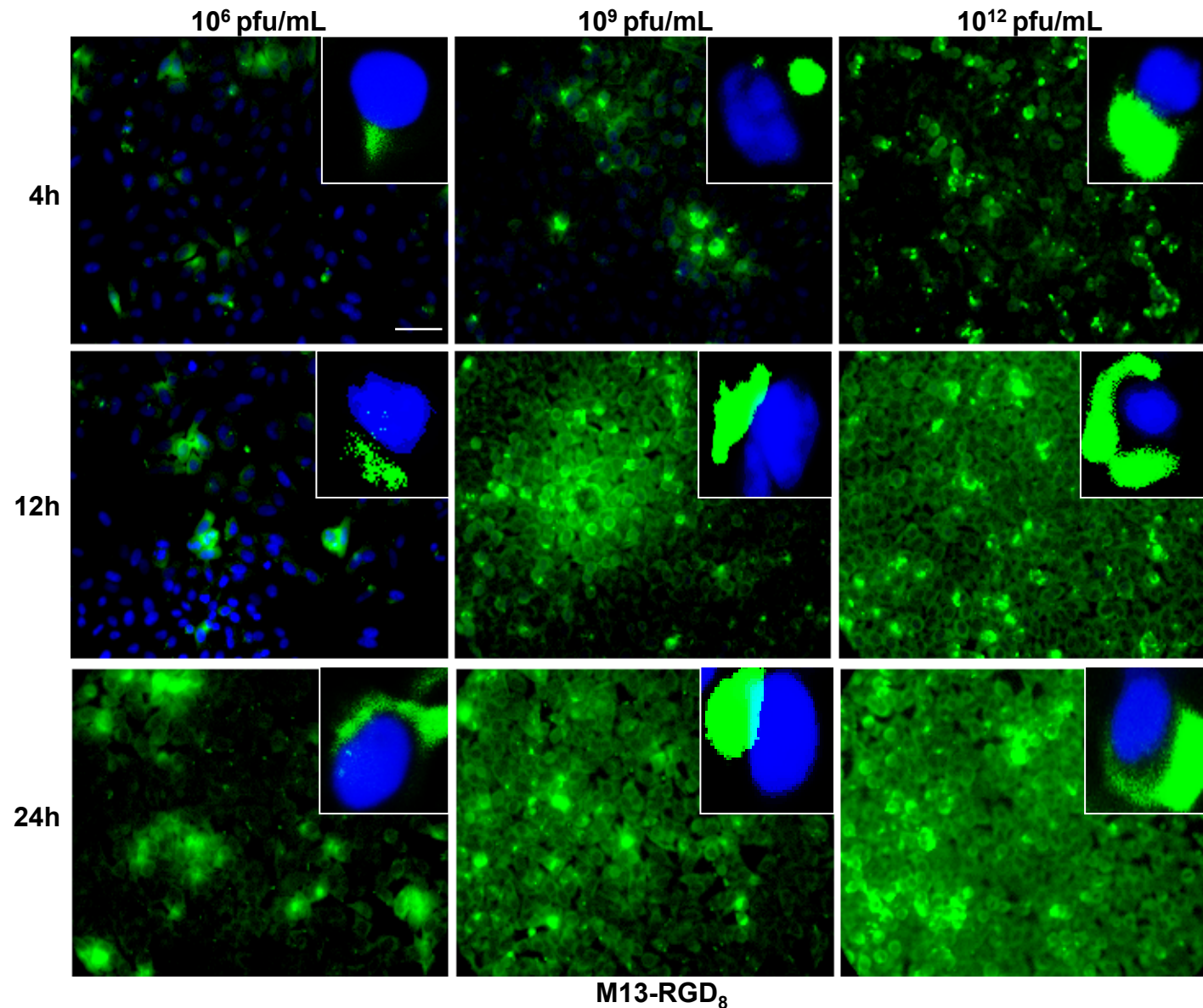
Fig. S2. M13-RGD$_8$ uptake is time and dose-dependent in HeLa cells. The time points of 4 h, 12 h and 24 h, and concentrations of 10^6, 10^9, and 10^{12} pfu/mL are shown. In all experiments, M13-RGD$_8$ was removed after 4 h of incubation with cells (see Methods). Blue, DAPI; Green, M13-RGD$_8$; 40x; inset, 100x.
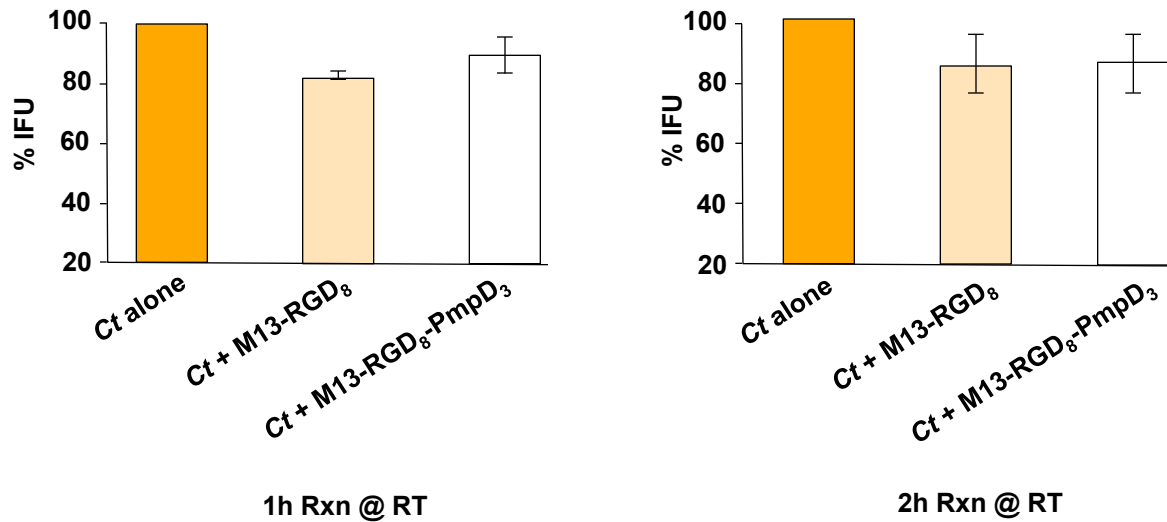
Fig. S3. Competition assay for M13-RGD$_8$, M13-RGD$_8$-PmpD$_3$ and *Ct* entry into HeLa cells. The experimental groups consisted of *Ct* infection alone, or M13-RGD$_8$ and M13-RGD$_8$-PmpD$_3$ incubated with *Ct* for 1 h or 2 h as indicated prior to infection of HeLa cells (see Methods). Independent experiments were performed in triplicate and normalized against the control.
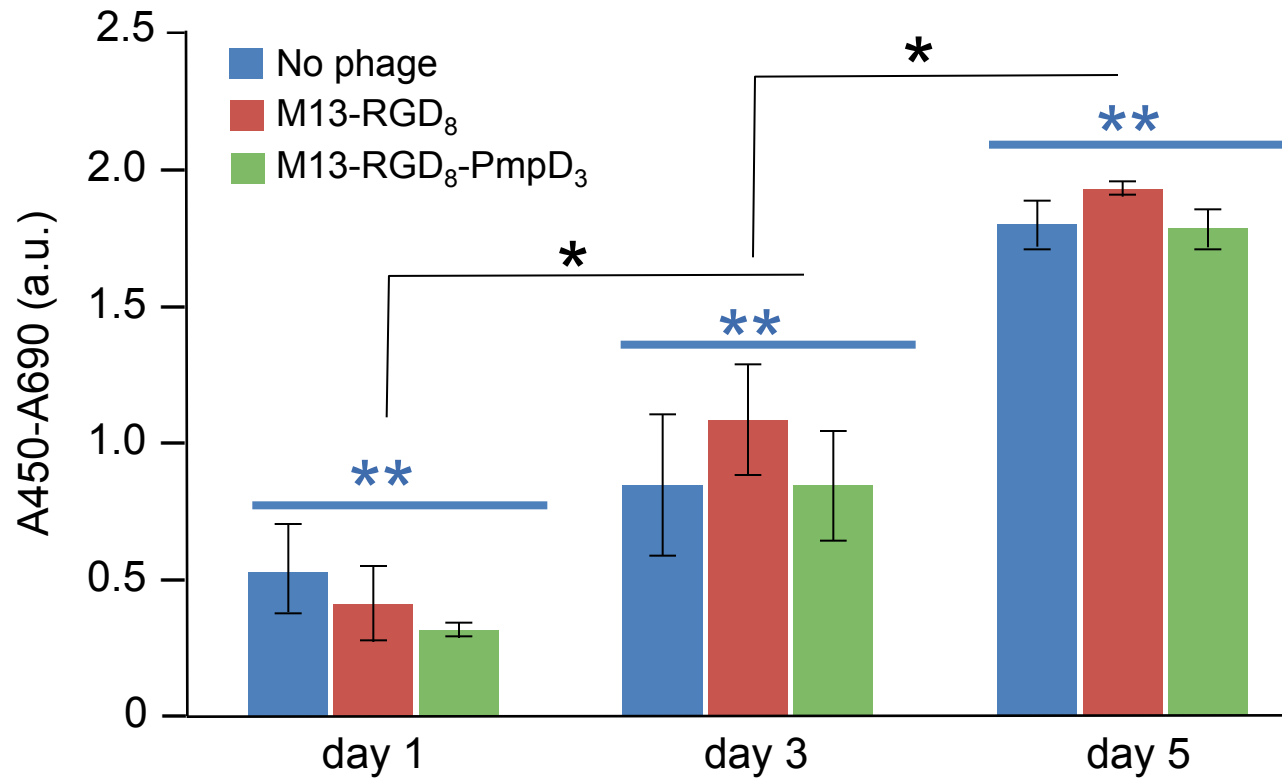
Fig. S4. *In-vitro* cell viability and proliferation test. HeLa 229 cells were treated with M13-RGD$_8$ or M13-RGD$_8$-PmpD$_3$ at a concentration of 10^{11} pfu/mL for various time points (days 1 to 5). At the end of exposure, cells were washed with PBS, and the WST-1 assay was performed (see Methods). Control cells cultured in phage-free media were performed at the same time. The data are expressed as ± mean SD of three independent experiments. *$p<0.05$, **$p<0.01$, (by two-way ANOVA).